PROGRESS IN COLOR, COLORANTS AND COATINGS

available online @ www.pccc.icrc.ac.ir

Progress in Color Colorants Coating 17 (2024), 297-306

Ministry of Science, Research and Technology
Institute for Color Science & Technology

Determination of Optimal Conditions for Dye Adsorption Using Hydrogel Containing Zinc Oxide and Carbon Quantum Dots by Experimental Design

P. Amoozadeh[1], A. H. Mohsen Sarrafi[1], B. Shirkavand Hadavand[*2], A. Niazi[1], E. Konoz[1]

[1.] Department of Chemistry, Central Tehran Branch, Islamic Azad University, P.O. Box: 146969-69191, Tehran, Iran.

[2.] Department of Resin and Additives, Institute for Color Science and Technology, P.O. Box: 16765-654, Tehran, Iran.

ARTICLE INFO

Article history:
Received: 07 Oct 2023
Final Revised: 21 Dec 2023
Accepted: 23 Dec 2023
Available online: 19 Feb 2024

Keywords:
Nanocomposite
Hydrogel
CQD
Rhodamine B
Dye adsorption
Experimental design

ABSTRACT

This research investigates the impact of pollutant degradation on the nanocomposite in the presence of ultraviolet light. In this study, the experimental design method was used to optimize the experimental conditions and analyze the removal of rhodamine B dye by the hydrogel/zinc oxide/carbon dots nanocomposite under ultraviolet light. The key parameters examined in this process are the amount of adsorbent (ranging from 0.25 to 1.5 g) and time (ranging from 30 to 135 min). The influence of pH on adsorption is disregarded due to its negligible effect. The analyses demonstrate a strong correlation between the predicted values and the experimental data. The study demonstrates the successful degradation mechanism under ultraviolet light. The results confirm the selection of degree 2 models based on a greater P-value at a confidence level above 95 %. The regression coefficient (R2 = 0.9454) validates the suitability of the model. The relationship between time and the adsorbent amount is investigated through response surface diagrams, revealing that an increase in both parameters leads to a higher percentage of removal. Consequently, the maximum removal is achieved at 135 min and 1.5 g of adsorbent. Furthermore, the contour diagram predicts the adsorption yield based on the amount of adsorbent and time. Overall, the results indicate that the use of the nanocomposite with ultraviolet light is an effective approach for pollutant removal. The removal percentage increases with longer exposure times and greater adsorbent amount. Prog. Color Colorants Coat. 17 (2024), 297-306© Institute for Color Science and Technology.

1. Introduction

In recent times, the textile industry has been generating a substantial amount of wastewater that contains a high concentration of pollutants, particularly dyes. The release of approximately 800,000 tons of dye into the environment annually has resulted in nearly 25 percent of these pollutants infiltrating the ecosystem through wastewater discharge [1, 2]. Even at low concentrations, the presence of these organic-colored substances in water adversely affects the biological activities of aquatic organisms and plants. Furthermore, these wastewaters possess carcinogenic and highly toxic properties, thereby necessitating the treatment of these colored wastewaters. Hence, the search for an effective method to address these pollutants is of utmost importance.

*Corresponding author: * shirkavand@icrc.ac.ir

https://doi.org/10.30509/pccc.2023.167208.1252

Several techniques, including adsorption, reverse osmosis, ultrafiltration, chlorination [3, 4], and biological approaches such as aerobic and anaerobic treatments [5], have been explored. Among these methods, the adsorption process stands out as a cost-effective, efficient, and straightforward means of eliminating color pollutants from wastewater.

Numerous adsorbents can be broadly categorized as natural or synthetic. However, to achieve enhanced adsorption and improved performance, different adsorbents have been developed and synthesized based on the dye materials' structure [6]. For instance, hydrogels serve as one such effective adsorbent. These hydrogels possess a three-dimensional structure comprising hydrophilic polymer chains [7]. Additionally, carbon nanoparticles can also be employed for pollutant removal. Notably, carbon nanoparticles feature oxygen-containing functional groups on their surface [8]. Also, carbon quantum dots have found various applications in different sectors [9-12]. The use of carbon quantum dots as an adsorbent can be considered.

Photocatalytic degradation serves as an extremely efficient method for the elimination of organic pollutants from wastewater, with the added advantage of converting these pollutants into harmless compounds like water and carbon dioxide [13, 14]. Zinc oxide represents one of the materials utilized in photocatalytic degradation due to its low cost, wide band gap, and high photocatalytic activity [15]. In the context of photocatalytic degradation, various factors, including temperature, pH, time, pollutant concentration, and adsorbent quantity, come into play and can significantly impact the efficiency of the photocatalytic degradation process [16-18]. Therefore, the identification of optimal conditions for pollutant removal is essential for saving both time and cost. Experimental design has proven to be one of the most effective methods for determining these optimal conditions [19, 20].

Response surface methodology (RSM) is a collection of mathematical and statistical techniques used for constructing empirical models and exploiting these models. RSM aims to establish a relationship between a response and the levels of various input variables or factors that influence it through the appropriate design and analysis of experiments. The response surfaces resulting from two-level factorial designs are modeled linearly, resulting in flat planes in three-dimensional space or twisted planes in the case of interactions. To monitor curvature in a response surface, a center point can be added to the two-factorial setup. If significant curvature is detected, smaller designs can be conducted within the existing levels or RSM can be employed. RSM can predict the response value under different process conditions. By applying RSM, it is possible to screen independent variables and identify the most significant main effect factors among several potential ones. Additionally, RSM can be used to identify non-identified interaction effects [21, 22].

This study aims to develop a suitable and efficient adsorption process for the removal of rhodamine B, a toxic wastewater pollutant, using a composite of hydrogel/nano zinc oxide/carbon quantum dots under ultraviolet light (UV). Furthermore, this study plans to determine the optimal conditions for adsorption through the utilization of the experimental design method.

2. Experimental

2.1. Materials

The urea, citric acid, sodium hydroxide, acrylamide, acrylic acid, benzophenone, triethanolamine, ammonium persulfate, zinc oxide, and rhodamine B dye were purchased from Merck (Germany). Trimethylolpropane triacrylate (TMPTA) was obtained from Aldrich Sigma (USA). All materials were used without purification.

2.2. Method

2.2.1. Synthesis of hydrogel/carbon quantum dots/nano zinc oxide

The synthesis was performed based on the method presented in the previous work [23], which is briefly mentioned below. First, carbon quantum dots and acrylic acid reacted with each other and then mixed well with acrylamide and acrylic acid, trimethylol-propane triacrylate, benzophenone, and triethanolamine and then cured using ultraviolet (UV) radiation.

2.2.2. Photocatalytic degradation of rhodamine B

According to scheme 1, the first 250 mL of 20 ppm solution of rhodamine B dye was prepared. Then the pH of the solution was adjusted to 8 with 0.5 molar sodium hydroxide solution and then 50 mL of the dye solution was poured into the flask and then the amount determined in the experimental design of the composite

adsorbent hydrogel/nano zinc oxide/carbon quantum dots was added to the solution and the solution was placed on a magnetic stirrer under UV light for the time determined in the experimental design until the adsorption was completely done and then for 10 min in a centrifuge with 4500 rpm and then the desired solution was filtered with filter paper and finally UV-Vis spectrum was taken from the resulting solution.

2.3. Instrumental methods

The sample was filtered by a Hettich Universal centrifuge (model PIT320, Germany). Spectroscopy of solutions containing dye was measured by Perkin Elmer UV spectrometer (model Lambda 950, USA). To adjust the pH of the samples, a METROHM pH meter (model 744, Switzerland) was used and the dye removal process was performed under a UVC - 15 w lamps from Osram Russia.

2.4. Experimental design

To investigate the effect of adsorbent amount and time on the adsorption rate, the experimental design method was used. The variables and their levels of change are presented in Table 1. Since the process of removing rhodamine B dye depends on different factors, it is necessary to identify and optimize them. Different optimization methods are used to obtain the ideal conditions for a process such as dye removal. The common optimization method is usually one factor at a time (OFOT). This optimization method requires a very large number of experiments, in which case the time and cost spent to obtain the optimal conditions of the process increases. Another drawback of this method is that only in case the initial values selected for the effective factors are close to the optimal conditions can be achieved. Another drawback of this method is not considering the interactions of the effective factors in the process on each other. Therefore, in recent years, experimental design methods have been used to optimize the effective factors in a process. Among these experimental design methods, the response surface method is used due to its ability to optimize processes in that several variables simultaneously affect the system response and each other. This method also takes into account the possible interactions between the factors in addition to the effect of the factors on the response (or responses). Therefore, we used one of the response surface methods called central composite design to optimize the conditions for removing rhodamine B dye by hydrogel/zinc oxide/ carbon quantum dots adsorbent in the laboratory. Among the response surface methods, two methods of central composite design and Box-Behnken have been used in most of the pollution removal processes, and we chose the central composite method. The effective factors in the process of dye removal by surface adsorption are pH, pollutant concentration, contact time between solution and adsorbent, and adsorbent amount. The factors studied based on preliminary experiments are A) contact time between dye and adsorbent (for obtaining maximum contact between adsorbent and dye) which was selected in the range of 30-135 min. B) The amount of adsorbent was considered in the range of 0.25-1.5 g. C) pH and since it did not affect adsorption, it was ignored and a constant value of 8 was set for all experiments.

The data obtained from the appropriate experiments by the central composite design were used to estimate the optimal conditions and regression model equation. The variables of time and amount of adsorbent and their range are given in Table 1. The levels of the parameters varied from -1 to +1 and the zero levels of the variables indicate the average values.

The results were analyzed using response diagrams and analysis of variance (ANOVA) in Design Expert Version 7.0 software. The specifications of the experimental design created and the response obtained from each of the designed experiments are given in Table 2.

Table 1: Levels of variables in RSM.

Variable	Label	Minimum (-1)	Mean (0)	Maximum (+1)
Absorbent (%)	A	0.25	0.625	1.5
Time (min)	B	30	52.5	135

Table 2: Designed conditions for dye removal and RSM responses.

Row	Test number	Absorbent (g)	Time (min)	Response dye absorption (%)
1	12	0.080	80.00	87.32
2	15	0.25	30.00	37.79
3	4	1.50	80.00	97.62
4	6	0.25	135.00	57.91
5	7	0.80	120.00	96.72
6	8	0.50	80.00	61.36
7	1	0.80	100.00	89.21
8	16	1.00	80.00	88.1
9	11	0.50	135.00	93.3
10	10	1.00	135.00	99.62
11	13	0.80	135.00	98.47
12	3	1.50	30.00	95.16
13	17	0.80	80.00	88.33

The responses presented in Table 2 pertain to the spectroscopy outcomes obtained from the samples after the completion of the photocatalytic degradation process. To achieve this, the spectroscopy of the samples was conducted based on the predetermined conditions determined by the experiment design software, encompassing the duration and weight of the adsorbent. Subsequently, a comparative analysis was carried out between the samples and the control sample, with the resulting data being documented in the table. The spectroscopy results of the samples can be observed in Figure 1.

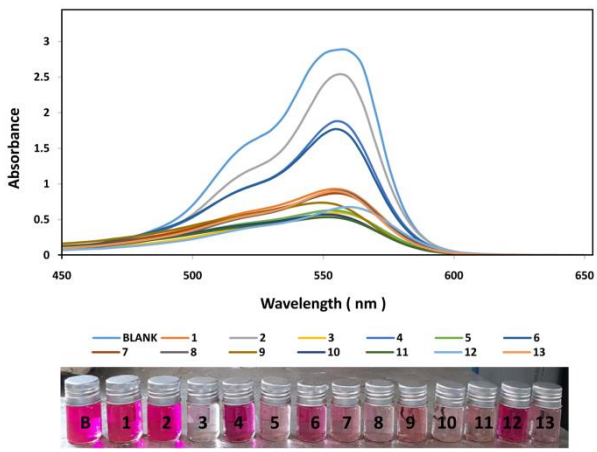

Figure 1: Spectroscopy results of samples based on experimental design.

3. Result and Discussion

3.1. FTIR characterization

In Figure 2 FTIR spectrum of hydrogel/zinc oxide/carbon quantum dot nanocomposite (HG/ZnO/CQD) is shown. Prominent absorption bands are observed in the hydrogel/zinc oxide/carbon quantum dot, including -OH stretching at 3640 cm^{-1}, C-O, C=C, and CH_2/CH_3 stretching at 1226 cm^{-1}, and visible bands at 1729 and 1411 cm^{-1}; the bands at 540 and 806 cm^{-1} represent Zn-O and doped nitrogen stretching vibrations, indicating a successful reaction [23-25].

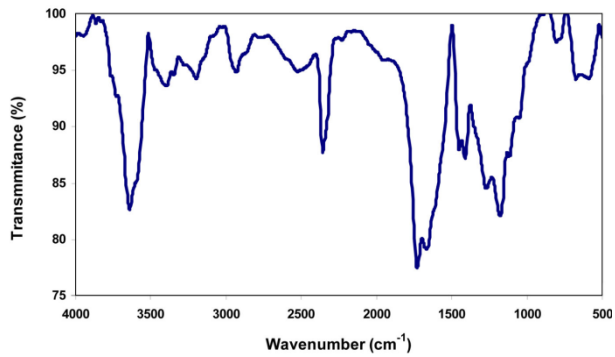

Figure 2: FTIR spectrum of hydrogel/zinc oxide/carbon quantum dot nanocomposite.

3.2. Experimental design results

After entering the response data in the design, the results are analyzed. This indicates that the data follow a normal distribution and therefore the responses obtained at present do not need any kind of initial preprocessing. The results of fitting the responses with the factors considered for the experiment are presented in Table 3. In Table 3, according to the P-value at a 95 % confidence level, two models have been proposed for modeling. Also in this table, a lack of fit tests has been presented for preliminary evaluation of the results. According to the results obtained (larger P-value at 95 % confidence level), the selection of model 2 is confirmed. The results of analysis of variance for model 2 response level are presented in Table 4.

The F-value of 26.36 and P-value of 0.0001 for the model indicate the suitability of the model used. This means that there is only a 0.03 % chance that this F-value is due to error. Regarding the P-value values for the main factors, second power, and interactions between the main factors, P-value values less than 0.05 (at 95 % confidence level) indicate that the effect of these factors on the response obtained is significant. According to the P-value values, it can be said that only the factors of contact time, adsorbent amount, and second power of adsorbent amount are important in the model. The P-value value of 0.0862 for lack of fit indicates that 8.62 % of lack of fit can be due to noise and therefore in the analysis of the variance table, the lack of fit factor is referred to as insignificant [26].

Considering the insignificance of the sentences containing the interactions between the main factors and the second power, the contact time returns to the modeling section, and the modeling is repeated by removing these sentences.

In regression, the most used statistic for evaluating the fit of a model is the regression coefficient (R^2), which shows how much of the variation in the response is explained by the model. The higher the R^2 is, the better the model fits the data. In this study, the regression coefficient is $R^2 = 0.9454$ (Table 4), which confirms the suitability of the model.

Finally, the values of correlation coefficient, adjusted correlation coefficient, and predicted correlation coefficient are obtained, which indicate the appropriate fit of the designed model with the presented data.

The value of (Adeq Precision) equal to 17.270 indicates a high signal-to-noise ratio in the constructed model and the prediction error value of 7185.63 also indicates the conformity of the model.

Table 3: Results of fitting responses with factors considered for experiment and lack of fit tests for evaluation of preliminary results.

Variable	Sum of squares	Degrees of freedom (df)	Mean square	F value	P value	Variable impact
Mean vs Total	91544.97	1	91544.97	-	-	-
Linearvs Mean	3710.22	2	1855.11	26.36	0.0001	Suggested
2FI vs Linear	3.62	1	3.62	0.047	0.8339	-
Quadratic vs 2FI	459.33	2	229.66	6.68	0.0239	-
Cubic vs Quadratic	237.89	4	59.47	61.58	0.0033	Suggested
Quartic vs Cubic	2.39	2	1.19	2.34	0.4196	Aliased
Residual	0.51	1	0.51	-	-	-
Total	95958.93	13	7381.46	-	-	-
Linear	703.23	9	78.14	153.19	0.0626	Suggested
2FI	699.61	8	78.45	171.46	0.0590	-
Quadratic	240.28	6	40.05	78.52	0.0862	-
Cubic	2.39	2	1.19	2.34	0.4196	Suggested
Quartic	0.000	0	-	-	-	Aliased
Pure Error	0.51	0	0.51	-	-	-

Table 4: Analysis of variance obtained from the results of experimental design.

variable	degrees of freedom (df)		mean square	F value	P value	Variable impact
Model	4173.17	5	834.63	24.26	0.0003	Significant √
A-Absorbent	2262.49	1	2262.49	65.77	0.0001<	-
B-Time	193.42	1	193.42	5.62	0.0495	-
AB	54.14	1	54.14	1.57	0.2499	-
A^2	448.13	1	448.13	13.03	0.0086	-
B^2	47.24	1	47.24	1.37	0.2796	-
Residual	240.79	7	34.40	-	-	-
Lack of Fit	240.28	6	40.05	78.52	0.0862	not significant
Pure Error	0.51	1	0.51	-	-	-
Cor Total	4413.96	12	-	-	-	-
Std. Dev.	5.87	-	R-Squared	0.9454	-	-
Mean	83.92	-	Adj R-Squared	0.9065	-	-
C.V. %	6.99	-	Pred R-Squared	0.6279	-	-
PRESS	7185.63	-	Adeq Precision	17.270	-	-
-2 Log Likelihood	74.84	-	BIC	90.23	-	-
	-	-	AICc	100.84	-	-

3.3. Comparison of theoretical and experimental data

From the results of theoretical and experimental data and according to the governing relations, it is clear that the removal percentage has a direct relationship with the amount of adsorbent and an inverse relationship with the second power of the amount of adsorbent. The removal percentage has an inverse relationship with the contact time. The order of the degree of influence of the sentences in the model is the second power of the amount of adsorbent and the contact time. The very small value of the estimated coefficient for the contact time sentence can support this theory that the contact time between the adsorbent and the dye does not have a high effect on the percentage of dye removal.

The relationship between the response (absorption percentage) and the independent variables (time and amount of adsorbent) in terms of coded factors and real factors are expressed by equations 1 and 2, respectively.

$$R1 = +88.87 +24.87\times A+8.22 \times B-5.04\times A \times B -19.26 \times A^2+4.95\times B^2 \quad (1)$$

$$R1 = +4.50122 +138.76779 \times \text{Absorbent}-5.22466E-003 \times \text{Time} -0.15372 \times \text{Absorbent} \times \text{Time}-49.30649 \times \text{Absorbent}^2 +1.79561E-003 \times \text{Time}^2 \quad (2)$$

In these relations, A and B are respectively the amount of adsorbent (weight percentage) and the adsorption time (min).

The examination of different curves of the model's fit with the data showed that the response data have a normal distribution and there is no need for pre-processing of the removal percentage data because the data are close to the straight line and there is no data outside the standard (correlation coefficient around 95 %) and a suitable linear regression model is observed (Figure 3) [27].

The curve of predicted values versus measured actual values (Figure 4) shows a uniform spread of points around the drawn straight line and the proximity of points to the drawn bisector indicates the high predictive power of the model.

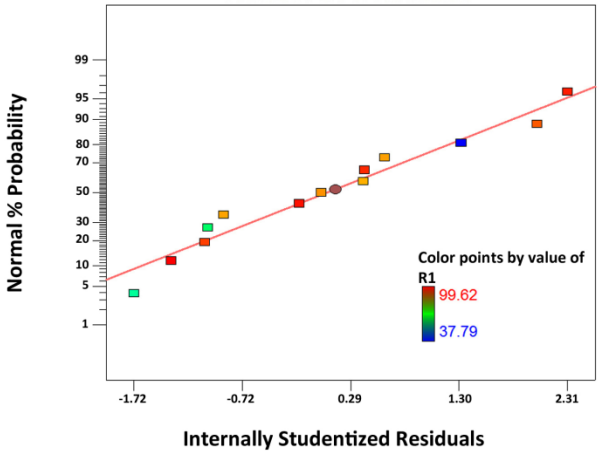

Figure 3: Scatter plot analysis in dye adsorption.

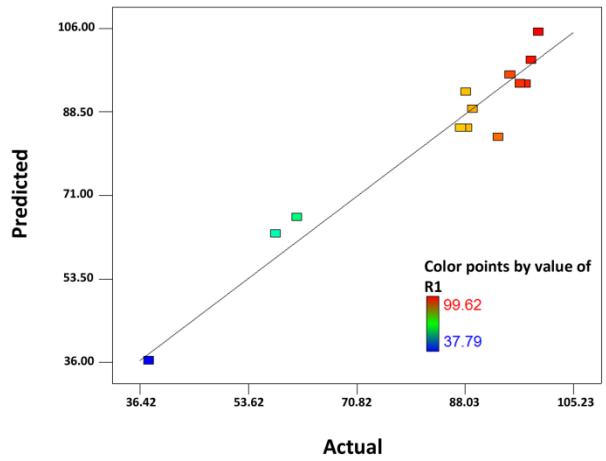

Figure 4: Plot of predicted values versus actual values.

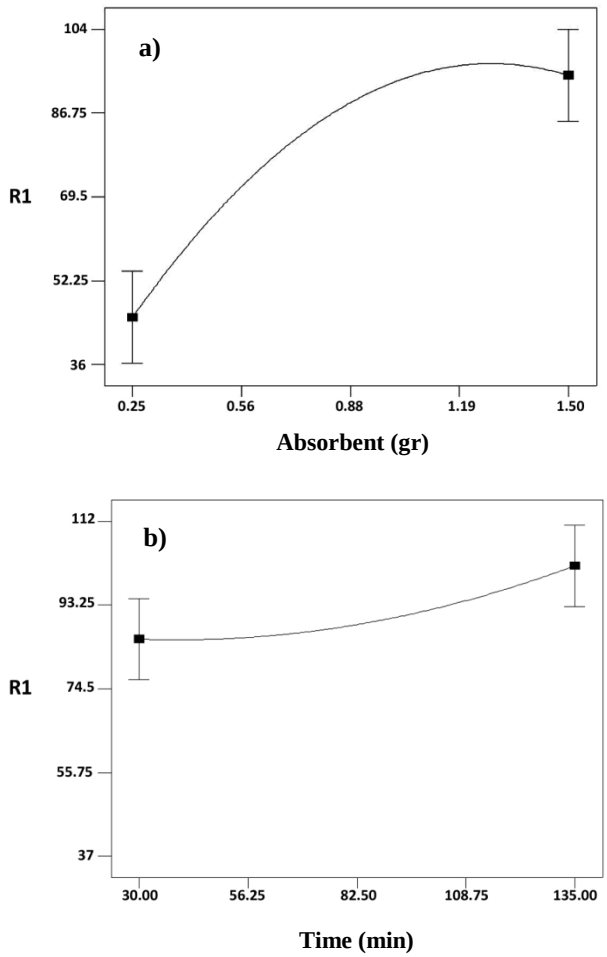

Figure 5: Dependence of time (a) and amount of adsorbent (b) on dye adsorption yield.

3.4. Dependence of effective characteristics on adsorption

Since the diagnostic parameters based on the residuals do not show us any statistical problem with the results, in the next step, the response surface plots have been investigated. In Figure 5, plots a and b show the dependence of time and amount of adsorbent, respectively. These plots show the increase of removal percentage with increasing time and amount of adsorbent. At 135 min, the highest amount of adsorption is observed and then the adsorption rate does not grow much (Figure 5 a). Figure 5 b shows the amount of adsorbent in dye adsorption, which has an ascending trend and reaches its maximum at 1.5 g. Therefore, by adding the amount of adsorbent, the adsorption process can be done faster and also increase the percentage of adsorption [28].

Using the model graphs, we can examine the type of impact of effective factors on the response. The 3D (Figure 6) and 2D (Figure 7) response surface plots for the improved regression model are shown. Figure 4 shows the effect of the adsorbent amount and time on the adsorption amount. The results obtained in this plot indicate that increasing time also has a positive effect on dye adsorption and more adsorption occurs. It is also clear that increasing the amount of adsorbent over time doubles the amount of adsorption

As mentioned before, the amount of adsorbent and reaction time are the main factors in the dye adsorption process. To better understand the interactions of these factors on adsorption yield and determine the optimal conditions for adsorption according to the results obtained, a contour plot was prepared and presented in Figure 7.

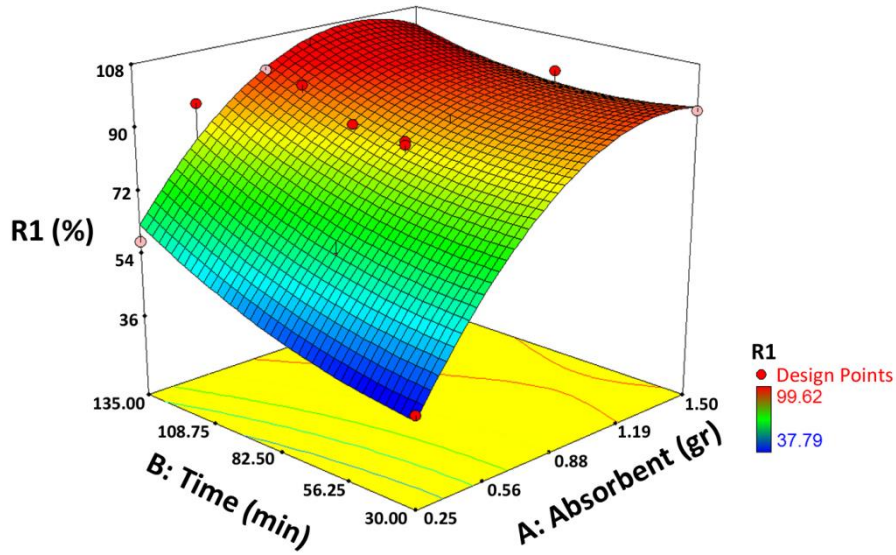

Figure 6: The 3D plot of effects of adsorbent amount (weight percentage) and adsorption time (min) on dye adsorption.

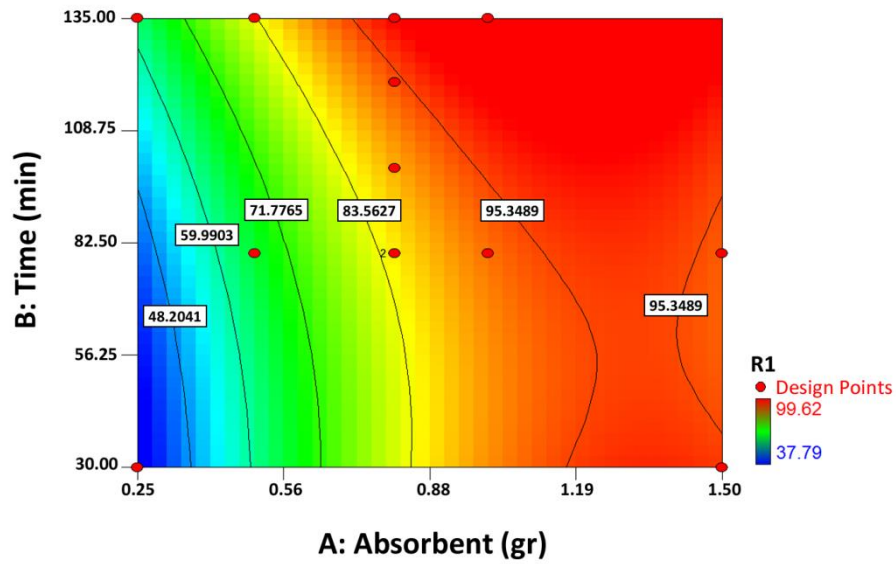

Figure 7: Contour plot of optimal conditions for dye adsorption

This plot shows their simultaneous interaction in the adsorption process in a desirable way. Based on the color guide that is specified on the left and top of the plot, as we get closer to the red areas, the percentage of dye removal increases, and as we move towards changing colors of yellow, green, and blue, we will reach areas where dye adsorption decreases. Therefore, with the help of this plot, we can determine the optimal conditions for adsorption, according to the importance of the amount of adsorbent and the length of time for adsorption. The curved lines in Figure 7 show the upper limit of numbers written on them for the adsorption amount and therefore for any hypothetical point desired by per-pendicularizing lines to both axes of the plot, we can obtain the conditions for forming this selected adsorption amount [29].

4. Conclusion

A composite material, comprising hydrogel, zinc oxide, and carbon quantum dots, was utilized as an adsorbent for the elimination of rhodamine B dye. FTIR

spectroscopy confirmed the successful synthesis of the composite material. The experimental design approach encompassed 13 experiments, wherein the responses were analyzed based on the obtained graphs. The primary factors influencing the removal of dye were the quantity of absorbent and the duration of contact, while the pH value remained constant at 8 and was determined using the experimental design technique to establish optimal conditions. The results obtained indicated a maximum absorption of 99.62 % for sample 10, which utilized 1 gram of absorbent and had a contact time of 135 minutes. Examination of the contour diagrams derived from the experiment revealed that to achieve an absorption efficiency exceeding 95 %, the quantity of adsorbent should exceed 1.1 grams. Furthermore, these diagrams can be employed to predict the efficiency value based on the absorbent quantity and absorption time.

Acknowledgements

We would like to thank the Institute for Color Science and Technology and Islamic Azad University, Tehran Central Branch for their support of this research.

5. References

1. Kumara NTRN, Lim A, Lim CM, Petra MI, Ekanayake P. Recent progress and utilization of natural pigments in dye-sensitized solar cells: A review. Renew Sustain Energy Rev. 2017; 78: 301-317. https://doi.org/10.1016/j.rser.2017.04.075.
2. Shindy HA. Fundamentals in the chemistry of cyanine dyes: A review. Dye Pigm. 2017; 145: 505-513. https://doi.org/10.1016/j.dyepig.2017.06.029.
3. Miklos DB, Remy C, Jekel M, Linden KG, Drewes J E, Hübner U. Evaluation of advanced oxidation processes for water and wastewater treatment: A critical review. Water Res.2018;139:118-131. https://doi.org/10.1016/j.watres.2018.03.042.
4. Cheremisinoff PN. Handbook of Water and Wastewater Treatment Technology: Butterworth–Heinemann: Oxford, UK. 2019.
5. Tetteh EK, Rathilal S. Kinetics and nanoparticle catalytic enhancement of biogas production from wastewater using a magnetized biochemical methane potential (MBMP) system. Catalysts. 2020; 10(10): 1200. https://doi.org/10.3390/catal10101200.
6. Wei F, Jawad Shahid M, Alnusairi GSH, Afzal M, Khan A, El-Esawi MA, Abbas Z, Wei K, Elahi Zaheer I, Rizwan M, Ali Sh. Implementation of floating treatment wetlands for textile wastewater management: A review. Sustainability. 2020; 12(14): 1-29. https://doi.org/10.3390/su12145801.
7. Gil E, Hudson S. Stimuli-responsive polymers and their bioconjugates, Prog Polym Sci. 2004; 29(12): 1173-1222.https://doi.org/10.1016/j.progpolymsci.2004. 08. 003
8. Manimegalai S, Vickram S, Raj Deena S, Rohini K, Thanigaivel S, Manikandan S, Subbaiya R, Karmegam N, Kim W, Govarthanan M. Carbon-based nanomaterial intervention and efficient removal of various contaminants from effluents - A review. Chemosphere. 2023; 312(1): 137319. https://doi.org/10.1016/j.chemosphere.2022.137319.
9. Madhi A, Shirkavand Hadavand B, Chemical treatment of cotton fabric by eco-friendly carbon quantum dots-chitosan nanocomposites. Appl Chem. 2022; 17(63): 55-66. https://doi.org/10.22075/CHEM.2021.23723.1988
10. Madhi A, Shirkavand Hadavand B, Bio-based surface modification of wool fibers by chitosan-graphene quantum dots nanocomposites. Iranian J Chem Chem Eng. 2022; 41(7): 2202-2212. https://doi.org/10.30492/ IJCCE.2021.527475.4657.
11. Madhi A, Shirkavand Hadavand B, UV protective bio-based epoxy/carbon quantum dots nanocomposite coatings: Synthesis and investigation of properties. J Compos Mater. 2022; 56(14): 2201-2210. https://doi.org/10.1177/00219983221092009.
12. Madhi A, Shirkavand Hadavand B, Fluorescent epoxy-graphene quantum dots nanocomposites: synthesis and study of properties. Polym-Plast Technol Mater. 2022; 61(2): 117-130. https://doi.org/10.1080/25740881.2021.1959929.
13. Raja S, Mattoso L H C. Functionalized polymer-based composite photocatalysts: Springer: Cham, Switzerland 2020.
14. Zhong J, Chen F, Zhang J. Carbon-deposited TiO_2: Synthesis, characterization, and visible photocatalytic performance. J Phys Chem C. 2010; 114: 933-939. https://doi.org/10.1021/JP909835M.
15. Chakrabarti S, Dutta B K. Photocatalytic degradation of model textile dyes in wastewater using ZnO as semiconductor catalyst. J Hazard Mater. 2004; 112(3): 269-278.https://doi.org/10.1016/j. jhazmat. 2004. 05. 013.
16. Tetteh E K, Rathilal S, Naidoo D B. Photocatalytic degradation of oily waste and phenol from a local South Africa oil refinery wastewater using response methodology. Sci Rep. 2020; 10: 1-12. https://doi.org/10.1038/s41598-020-65480-5.
17. Gopinath KP, Madhav N V, Krishnan A, Malolan R, Rangarajan G. Present applications of titanium dioxide for the photocatalytic removal of pollutants from water: A review. J Environ Manag. 2020; 270: 110906.https://doi.org/10.1016/j.jenvman.2020110906.
18. Rodrigues CSD, Madeira LM, Boaventura R AR. Optimization of the azo dye Procion Red H-EXL

degradation by Fenton's reagent using experimental design. J Hazard. Mater. 2009;164: 987-994. https://doi.org/10.1016/j.jhazmat.2008.08.109.
19. Ounas O, Lekhlif B, Jamal-Eddine, J. Effect of three operating variables on degradation of direct blue 199 by TiO_2 immobilized into a polymer surface: response surface methodology. Prog Color Colorants Coat. 2021;14(3):161-178. https://doi.org/10.30509/ PCCC. 2021.81711.
20. Shirkavand Hadavand B, Saeb MR, Najafi F, Malekian AR. Response surface analysis for understanding the effects of synthesis parameters on the microstructure of hyperbranched polyesters. J Macromol Sci A. 2016; 53(12): 741-749. https://doi.org/10.1080/10601325.2016.1237812.
21. Mehrizad A, Gharbani P. Removal of methylene blue from aqueous solution using nano-TiO_2/UV process: optimization by response surface methodology. Prog Color Colorants Coat. 2016; 9: 135-143. https://doi.org/10.30509/PCCC.2016.75878.
22. Ounas O, Lekhlif B, Jamal-Eddine J. Effect of three operating variables on degradation of Direct Blue 199 by TiO_2 immobilized into a polymer surface: Response surface methodology. Prog Color Colorants Coat. 2021; 14: 161-178. https://doi.org/ 10.30509/ PCCC.2021.81711.
23. Amoozadeh P, Mohsen Sarrafi A.H, Shirkavand Hadavand B, Niazi A, Konoz E. UV-curable hybrid hydrogels of carbon quantum dots: synthesis, characterizations and investigation of properties and rheological behavior. Polym-Plast Technol Mater. 2022; 61(18): 2063-2072.https://doi.org/ 10.1080/ 25740881.2022.2089580.
24. Wu S, Zhou C, Ma C, Yin Y, Sun C., Carbon quantum dots-based fluorescent hydrogel hybrid platform for sensitive detection of Iron ions. J Chem. 2022; 3737646: 1-14. https://doi.org/10.1155/ 2022/ 3737646.
25. Yan X, Rahman S, Rostami M, Tabasi Z A, Khan F, Alodhayb A, Zhang Y, Carbon quantum dot-incorporated chitosan hydrogel for selective sensing of Hg^{2+} ions: Synthesis, characterization, and density functional theory calculation. ACS Omega. 2021; 36: 23504-23514. https://doi.org/10.1021/acsomega. 1c03557.
26. Ilomuanya MO, Amenaghawon NA, Odimegwu J, Okubanjo OO, Aghaizu C, Oluwatobiloba A, Akimien T, Ajayi T, Formulation and optimization of gentamicin hydrogel infused with tetracarpidium conophorum extract via central composite design for topical delivery. Turkish J Pharmac Sci. 2018; 15(3): 19-27. https://doi.org/10.4274/tjps.33042.
27. Heidari S, Esmaeilzadeh F, Mowla D, Ghasemi S, Optimization of key parameters affecting swelling capacity of poly(acrylamide-co-acrylic acid) hydrogels in salt water using response surface methodology (RSM). J Macromol Sci Part B Phys. 2021; 60(12): 971-988. https://doi.org/10. 1080/ 00222348.2021.1932950.
28. Bagheri R, Ghaedi M, Asfaram A, Alipanahpour Dil E, Javadian H, RSM-CCD design of malachite green adsorption onto activated carbon with multimodal pore size distribution prepared from Amygdalus scoparia: Kinetic and isotherm studies. Polyhedron, 2019; 171: 464-472. https://doi.org/10.1016/ j.poly. 2019.07.037.
29. Zhao W, Hao C, Guo Y, Shao W, Tian Y, Zhao P, Optimization of adsorption conditions using response surface methodology for tetracycline removal by $MnFe_2O_4$/multi-wall carbon nanotubes. Water. 2023; 15(13): 1-17. https://doi.org/10.3390/w15132392.

How to cite this article:
Amoozadeh P, Mohsen Sarrafi AH, Shirkavand Hadavand B, Niazi A, Konoz E. Determination of Optimal Conditions for Dye Adsorption Using Hydrogel Containing Zinc Oxide and Carbon Quantum Dots by Experimental Design. Prog Color Colorants Coat. 2024;17(3):297-306. https://doi.org/10. 30509/pccc.2023.167208.1252.